On the use of lithogenic tracer measurements in aerosols to constrain dust deposition fluxes to the ocean southeast of Australia

Claudia Hird[1,★], Morgane M. G. Perron[1,2,★], Thomas M. Holmes[3,★], Scott Meyerink[3],
Christopher Nielsen[1], Ashley T. Townsend[4], Patrice de Caritat[5], Michal Strzelec[1], and
Andrew R. Bowie[1,3]

[1]Institute for Marine and Antarctic Studies (IMAS), University of Tasmania, Battery Point, Tasmania, Australia
[2]Univ. Brest – UMR6539 UBO/CNRS/IRD/IFREMER, LEMAR, IUEM, Plouzané, France
[3]Australian Antarctic Program Partnership (AAPP), University of Tasmania, Battery Point, Tasmania, Australia
[4]Central Science Laboratory, University of Tasmania, Hobart, Tasmania, Australia
[5]John de Laeter Centre, Curtin University, Bentley, Western Australia, Australia
★These authors contributed equally to this work.

Correspondence: Morgane M. G. Perron (morgane.perron@univ-brest.fr)

Abstract. Australia contributes a significant amount of dust-borne nutrients (including iron) to the Southern Ocean, which can stimulate marine primary productivity. A quantitative assessment of the variability in dust fluxes from Australia to the surrounding ocean is therefore important for investigating the impact of atmospheric deposition on the Southern Ocean's carbon cycle. In this study, lithogenic trace metals (aluminium, iron, thorium, and titanium) contained in aerosols collected between 2016 and 2021 from kunanyi / Mount Wellington in lutruwita / Tasmania (Australia) were used to estimate dust deposition fluxes. Lithogenic fluxes were calculated using each tracer individually, as well as an average using all four tracers. This latter approach enabled an assessment of the uncertainty associated with flux calculations using only individual tracers. Elemental ratios confirmed the lithogenic nature of each tracer in aerosols when compared with both Australian soil samples and the average Earth's upper continental crust. Lithogenic flux estimates showed annual dust deposition maxima during the austral summer, following the Australian dust storm season, and annual minimum deposition flux over winter. The data provided here will help to constrain model estimates of Southern Hemisphere atmospheric deposition fluxes and their subsequent impact on global ocean biogeochemical cycles.

1 Introduction

Lithogenic mineral particles such as iron oxyhydroxides, kaolinite, illite, and smectite are commonly entrained into the atmosphere (Cudahy et al., 2016) following the erosion of the Earth's upper continental crust (UCC) (Crawford et al., 2021). Such dust particles are the primary source of trace metals including aluminium (Al), iron (Fe), thorium (Th), and titanium (Ti) to the atmosphere, which can therefore be used as tracers of aeolian lithogenic inputs to the ocean (Baker et al., 2020). Dust carries important nutrients, includ-

ing Fe, to marine ecosystems, feeding primary producers (Mackie et al., 2008). Due to the current lack of field observations on the concentrations of aeolian trace metals and their corresponding dust deposition fluxes, large uncertainties remain regarding how and to what extent the dust supply fertilises key oceanic regions such as the Southern Ocean with vital nutrients. This leads to a poor understanding of the impact of dust deposition on the biological carbon pump.

The amount of dust entrained into the atmosphere depends on soil surface roughness, vegetation and coverage, particle size, composition and moisture content, and local conditions

such as wind speed and rainfall, which change both regionally and seasonally (Mahowald et al., 2009). Air masses can carry dust over thousands of kilometres before particles return to land or fall onto the surface ocean (Mackie et al., 2008). Atmospheric deposition of dust to the open ocean has been demonstrated to act as a key supplier of vital macro- and micro-nutrients (such as Fe) to the marine ecosystem (Mackie et al., 2008; Weis et al., 2024). For example, during the austral summer in 2019–2020, nutrient supply from large dust-containing bushfire emissions (Perron et al., 2022; Hamilton et al., 2022) was identified as the main trigger of a large and long-lasting phytoplankton bloom in the South Pacific Ocean (Weis et al., 2022).

Field and modelling approaches to estimating dust deposition both offer various benefits and drawbacks. Field observations at sea are influenced by local environmental conditions (i.e. weather and surface ocean properties) and are not representative of the large-scale or long-term atmospheric deposition trends (Anderson et al., 2016). Time series stations on land can overcome the issue of temporal coverage but may not be representative of atmospheric loading and deposition over remote oceanic regions. To date, global models are not capable of reproducing atmospheric concentrations of trace metals transported in dust to remote areas and cannot accurately quantify particle settling rates (Anderson et al., 2016). Considering the Southern Hemisphere, model estimates tend to overestimate total dust emission at the source and underestimate soluble trace element deposition fluxes over the ocean (Anderson et al., 2016; Ito et al., 2020). To reduce uncertainty in dust deposition fluxes to the open ocean, it is essential to validate model fluxes using field-based observations. Long-term atmospheric observatories, particularly near the coasts, are attracting increasing interest from the scientific community as a tool to better understand seasonal to interannual patterns of deposition events in addition to shipboard observations and satellite estimates (Perron et al., 2022; De Deckker, 2019).

In Australia, the large spatial heterogeneity of soil types and the highly episodic nature of weather events such as droughts, bushfires, and dust storms make it particularly difficult to model dust deposition fluxes (Mackie et al., 2008), though modern dust emissions from South Australia have been observed as far as the snow sheet of inner Antarctica (Vecchio et al., 2024). A main source of trace metals to the Australian sector of the Southern Ocean is dust carried from the kati thanda / Lake Eyre and dhungala–barka / Murray–Darling geological basins (De Deckker, 2019). The typical dust storm season in Australia spans from September to November (austral spring), with the most extreme storms occurring in September (O'Loingsigh et al., 2017). The dust season can extend through the austral summer due to bushfires (and postfire unvegetated ground) across southern Australia (Hamilton et al., 2022). In a study conducted by Perron et al. (2022), atmospheric concentrations of mineral dust and associated lithogenic tracers (Al, Fe, and Ti) were reported to

be 2.5-fold higher, on average, during fire events compared to days not impacted by bushfires in lutruwita / Tasmania, Australia.

Dust deposition fluxes reported by different models range over an order of magnitude (from 0.55 to 5.48 mg m^{-2} d^{-1}) over the Southern Ocean region southeast of Australia (Mahowald et al., 2005; Weis et al., 2024). Different methods have also been used to estimate dust deposition fluxes from field samples. While broadly used in air pollution studies (Bindu et al., 2016), total aerosol loading measurements based on gravimetry does not enable the discrimination of atmospheric sources (e.g. dust vs. anthropogenic). In addition, such a method is not compatible with atmospheric trace metal studies, where a strict protocol requires minimal filter handling to prevent contamination from the analysis of a single-tracer element, for example, Al or Th, in aerosol samples and in seawater (Anderson et al., 2016). However, single-element dust flux estimates are subject to anomalous data stemming from contamination, deviation from the mean UCC, or preferential mineralisation following a particular laboratory protocol. Recently, the analysis of four lithogenic tracers (namely, Al, Fe, Th, and Ti) in marine sinking particles collected at the Southern Ocean Time Series (SOTS) mooring station (47° S, 140° E) were used to calculate an average "multi-tracer" estimate of dust deposition fluxes to surface waters of the subantarctic ocean south of Australia (Traill et al., 2022). The latter field-based flux estimates showed good agreement with remotely sensed proxies for dust transport and modelled deposition estimates. Elemental ratio analysis in the same sediment trap samples suggested that lithogenic material from southeastern Australia was the most likely source of Al, Fe, Th, and Ti to this area of the Southern Ocean (Traill et al., 2022).

In this study, the analysis of the same four lithogenic tracers (Al, Fe, Th, and Ti) was performed in aerosol samples collected at the kunanyi / Mount Wellington time series sampling station in southern lutruwita / Tasmania (Australia). Dust deposition fluxes were estimated from both individual tracer concentrations and using the multi-tracer approach used by Traill et al. (2022). Here we report a 5-year (2016–2021) time series of dust deposition flux estimates downwind of the southeastern Australian dust path, which is at one of the gateways to the Southern Ocean. The suitability of the four metals as lithogenic tracers was also verified by comparing elemental ratios (relative to Al) in the aerosol samples to the average topsoil composition in Australia (this study) and to the averaged UCC composition (McLennan, 2001).

2 Material and methods

2.1 Aerosol collection and study site

kunanyi / Mount Wellington overlooks Hobart, the capital city of the Australian island state of lutruwita / Tasmania. The mountain is in a strategic position for sampling

one of the three major atmospheric pathways in Australia (Baddock et al., 2015; Bowler, 1976), where air masses from mainland Australia are transported southeastwards over lutruwita / Tasmania (and our sampling site; Fig. 1) before reaching the Southern Ocean. This study uses aerosol filters collected on a HiVol 3000 air particulate sampler (Acoem Australasia (Ecotech Pty Ltd), Melbourne, Australia) positioned at 1271 m above sea level on the summit of kunanyi / Mount Wellington. Filter samples have been collected for total suspended particulates (TSPs) since September 2016, with each sample representing a period ranging from a few days to 2 weeks, depending on weather conditions and specific weather events, and allowing for sampler servicing and calibration. Samples suspected of contamination or that were significantly wet at the time of recovery were discarded, and sampling was suspended in the wintertime of the years 2017, 2018, and 2019 for operational reasons. As a result, 125 aerosol samples were selected from the kunanyi / Mount Wellington atmospheric time series collection for this study (November 2016–February 2022). The origin and concentration of aerosol Fe in 80 samples from this dataset was previously reported in Perron et al. (2022); however, the present study differs in using total concentrations of Fe, Al, Th, and Ti to calculate atmospheric (dust) deposition fluxes and the associated seasonal and interannual trends at the sampling station.

2.2 Aerosol leaching protocol

Laboratory work for aerosol and soil sample processing (Sect. 2.2 and 2.3) followed procedures recommended by GEOTRACES for ultra-trace sampling and analysis (Cutter et al., 2017). All reagents were ultra-high purity (UHP) and either purchased (Baseline, SeaStar Chemicals) or distilled in-house using instrument quality reagents (IQ grade, SeaStar Chemicals). Whatman W41 (203 mm × 254 mm paper sheets; Sigma-Aldrich) filters were acid-washed in a series of 24 h hydrochloric acid (0.5 M HCl) baths and rinsed with UHP water to leach any impurities and reduce the impact of the cellulose filter on the analysis of trace elements in aerosols (Perron et al., 2020a).

Perron et al. (2020a) suggested a three-step leaching method to define trace metal concentrations and solubility in aerosols taken from land-based stations in Australia (Strzelec et al., 2020a, b) and on research vessels operating around Australia and in the Southern Ocean (Perron et al., 2020b, 2021). Although samples were collected and analysed in batches over several years, the collection and analysis of each batch of samples follow the same protocol, and the resulting data were quality-controlled against blanks, replicate analysis, and certified reference materials (Table S1 in the Supplement).

One sub-sample of 47 mm diameter was cut off each aerosol filter sheet collected at our sampling station using a sharp titanium punch cutter (Perron et al., 2020a).
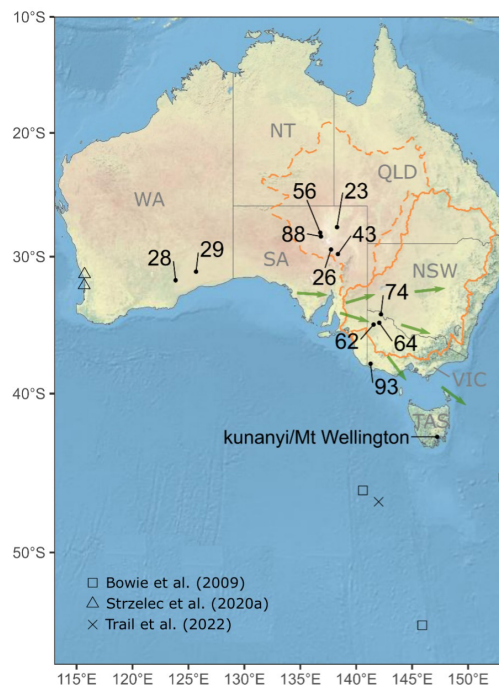

Figure 1. Location of the aerosol sampling station at kunanyi / Mount Wellington in Tasmania (TAS). Black dots display the locations of selected NGSA soil samples in the Australian states of Western Australia (WA), South Australia (SA), and Victoria (VIC), with identification numbers annotated (see Table S2). Prevailing dust pathways of southeast Australia are displayed as green arrows, as adapted from Sprigg (1982) and Mackie et al. (2008). The kati thanda / Lake Eyre (dashed line) and dhungala–barka / Murray–Darling (solid line) geological basins are delineated in orange. Location of previous field studies that estimated dust deposition fluxes are also indicated.

Sub-samples were successively leached using UHP water (Milli-Q®; 18.2 MΩ) and 1.1 M ammonium acetate (10 mL; pH 4.7). The remaining filter residue was then digested using a mixture of concentrated nitric acid (HNO_3; 1 mL) and concentrated hydrofluoric acid (HF; 0.25 mL) at 120 °C for 12 h (Perron et al., 2020a). The sum of all three steps in the protocol provided the total concentration data for each lithogenic tracer in aerosols which is used in this study (Perron et al., 2020a). Satisfactory recoveries (> 90 %) were obtained for Al, Fe, and Ti when applying the total metal digestion step of the protocol to two reference materials, namely Arizona Test Dust (ATD) (Morton et al., 2013) and the GeoPT13-certified Koeln loess (International Association of Geoanalysts) (Potts et al., 2003) (Table S1). A smaller recovery of 87 % (using only certified reference material) obtained for Th highlights the unique extraction and stability chemistry of the metal which our protocol is not optimised for. Thorium concentrations are therefore likely to be slightly underestimated in this study, as discussed in Sect. 3. Only total metal concentrations are discussed in the present study.

2.3 Atmospheric deposition flux estimates

The total concentration of each lithogenic tracer in our samples was used to calculate single-tracer dust deposition flux estimates. Additional measurements on the collected aerosols (e.g. carbon and major ion analysis) were not available for this study, so an intrinsic calculation of the total aerosol mass on each individual aerosol filter using these parameters was not possible.

In addition, due to the lack of necessary meteorological data to estimate particle deposition velocities specific to our study site, a single coarse-particle deposition velocity of $0.2 \, \mathrm{cm \, s^{-1}}$ was applied to trace-metal-bearing dust deposition estimates, based on the literature in similar study regions (Baker et al., 2017; Perron et al., 2020b; Winton et al., 2016b). In this study, "$F_{(X)}$" denotes the deposition flux estimate for the individual lithogenic tracer "X". $F_{(X)}$ (in $\mathrm{mg \, m^{-2} \, d^{-1}}$) was obtained following Eq. (1):

$$F_{(X)} = C_x \times V_d, \tag{1}$$

where X is the lithogenic tracer, i.e. Al, Fe, Th or Ti; C_x is the total metal concentration ($\mathrm{ng \, m^{-3}}$) in aerosols; and V_d is a constant deposition velocity of $1723 \, \mathrm{m \, d^{-1}}$ ($0.2 \, \mathrm{cm \, s^{-1}}$). It should be mentioned that uncertainty with a factor of 3 was previously attributed to the use of a set deposition velocity as it does not account for specific particle size in different aerosol samples or for specific atmospheric conditions such as humidity and wind speed at the collection time (Baker et al., 2016; Winton et al., 2016b; Duce et al., 1991).

Similar to other studies reported in the literature, a single-tracer dust (lithogenic) deposition flux estimate, $F_{\mathrm{Lith}(X)}$, was calculated by dividing $F_{(X)}$ by the average abundance ($[X]_{\mathrm{UCC}}$, wt %) of the element X in the UCC as reported in McLennan (2001), so that Al $= 8.04 \%$, Fe $= 3.5 \%$, Th $= 1.07 \times 10^{-3} \%$, and Ti $= 0.41 \%$, following Eq. (2).

$$F_{\mathrm{Lith}(X)} = \frac{F_{(X)} \times 100}{[X]_{\mathrm{UCC}}} \tag{2}$$

While $F_{\mathrm{Lith}(X)}$ estimates are solely based on the analysis of a single-lithogenic tracer, a multi-tracer dust deposition flux estimate, F_{LithAv}, was obtained by calculating the average of all four $F_{\mathrm{Lith}(X)}$ (Eq. 3; $N = 4$) for each individual aerosol sample.

$$F_{\mathrm{LithAv}} = \frac{\sum F_{\mathrm{Lith}(X)}}{N} \tag{3}$$

Multi-tracer F_{LithAv} estimates were calculated using both the reported average UCC composition (McLennan, 2001) and Australian soil measurements (see Sect. 2.4 in this study) as references for comparison.

2.4 Soil sampling and processing

In total, 11 topsoil (0–10 cm) samples were selected from the National Geochemical Survey of Australia (NGSA)

Project, Geochemical Atlas of Australia (Geoscience Australia), which is a continental-scale geochemical survey covering most of Australia (de Caritat and Cooper, 2011; de Caritat, 2022).

In this study, soil samples originating from the southern part of Western Australia, from South Australia, and from Victoria were selected and analysed (Fig. 1) as they likely better represent particles entrained through the southeast Australian dust path towards our sampling station and the Southern Ocean (Baddock et al., 2015; Fig. S1). These sources include the geological basins of kati thanda / Lake Eyre and dhungala–barka / Murray–Darling. It should be mentioned that no sample from New South Wales was used for this study, although a large part of the dhungala–barka / Murray–Darling basin is located in this state.

In total, 10 mg of each soil sample were dry sieved through a 63 µm nylon screen to capture the soil fraction fine enough to be entrained into the atmosphere (Strzelec et al., 2020a). The sieved fraction was then processed through the same sequential leaching method described in Sect. 2.2 (Perron et al., 2020a). Aerosol and soil leachates were analysed for a suite of elements, including Al, Fe, Th, and Ti, by high-resolution (sector field) inductively coupled plasma mass spectrometry (HR-ICP-MS; Thermo Fisher Scientific Element 2) at the Central Science Laboratory of the University of Tasmania. Increased spectral resolution was employed to resolve major spectral interference overlaps associated with analysis of Al, Fe, and Ti. Further details on the ICP-MS analysis procedure are provided in Perron et al. (2020a).

2.5 Atmospheric source tracking

The ratio between the total concentration of each lithogenic tracer of interest, $T(X)$, and the total Al concentration, $T(\mathrm{Al})$, in individual aerosol samples was calculated and compared to the same ratio in the average UCC reported in McLennan (2001) and in the average topsoil from southeastern Australia (Sect. 2.3). The so-called enrichment factor (EF; Eq. 4) was used to ascertain the lithogenic origin of Fe, Th, and Ti in this study.

$$\mathrm{EF} = \frac{\frac{C_x}{C_{\mathrm{Al}}} \, \mathrm{aerosol}}{\frac{C_x}{C_{\mathrm{Al}}} \, \mathrm{UCC}} \tag{4}$$

Using this approach, an EF value below 10 was considered to indicate a prevailing lithogenic source origin for the metal tracers, while an EF exceeding the threshold value of 10 is associated with an enrichment from non-lithogenic atmospheric sources such as anthropogenic combustion (Shelley et al., 2015; Perron et al., 2022). Reimann and de Caritat (2005) warned about the biases associated with using a low EF threshold to identify anthropogenic sources due to the natural variability in the Earth's crust composition, fractionation of elements during their emission to – and transport within – the atmosphere, and biogeochemical processes dur-

Table 1. Comparison of mean Al, Fe, Th, and Ti concentrations measured (parts per million, ppm) in Australian soil samples ($n = 11$) compared to concentrations reported in the average UCC by McLennan (2001). Enrichment factors (EFs) calculated for Fe, Th, and Ti (using Al as a reference) in aerosols collected at kunanyi / Mount Wellington ($n = 125$) are also displayed using both crustal references.

	UCC	Australian soils	kunanyi / Mount Wellington aerosols		
				UCC	Australian soil
Al	80 400	38 560			
Fe	35 000	22 616	EF(Fe)	1.6 ± 0.6	1.2 ± 0.5
Th	10.7	10.3	EF(Th)	1.3 ± 2.5	0.7 ± 1.2
Ti	4100	4313	EF(Ti)	1.2 ± 0.6	0.6 ± 0.6

ing and after aeolian transport. Here, a high EF threshold of 10 is adopted to account for such variability.

3 Results and discussion

3.1 Evaluating the lithogenic origin of the four tracers in aerosols

Enrichment factors (EFs) were calculated for Fe, Th, and Ti measured in aerosols and compared to the Australian soil samples selected from the NGSA (this study) and then compared to the averaged UCC composition from McLennan (2001) (Table 1). Calculated EF values were used to discard significant contributions of non-lithogenic sources to our lithogenic tracers in kunanyi /Mount Wellington aerosols, as indicated by EF > 10.

Overall, EFs close to 1 were measured for all aerosol samples, suggesting that the lithogenic tracers used in this study are indeed of a prevailing crustal origin. Using Australian soil concentration (Tables 1 and S2) to calculate EFs resulted in values further away from the threshold of 10. In particular, EFs calculated using Australian soil data are closer to 1 for Fe and Th when compared to using average UCC values (McLennan, 2001). Indeed, underestimated Th measurements due to incomplete sample digestion (Sect. 2.2) in our study result in a similar underestimate of EF. The elemental ratio of Ti / Al in aerosol samples collected at kunanyi / Mount Wellington (Fig. 2) was closer to the average ratio of the UCC, resulting in EF(Ti) closer to 1 when compared to using average Australian soil measurement as a reference.

Mean Al and Fe concentrations measured in our Australian soil samples were both two times smaller than the average UCC values reported by McLennan (2001), while Ti and Th concentrations were similar within 10 % (Fig. 2 and Table S2). While Australian soil is known for its high Fe content (Mahowald et al., 2009; Strzelec et al., 2020a),

a high soil heterogeneity across this vast country may explain such surprising observation. This resulted in calculated Th / Al and Ti / Al ratios higher for Australian soil samples, while Fe / Al ratios remained similar compared to the average UCC.

Elemental ratios calculated for individual aerosol samples are summarised in the Table S4. Both Fe / Al and Ti / Al ratios showed a clear seasonal trend, with higher ratios resembling mean ratios measured in Australian soil samples (Fe / Al = 0.59 and Ti / Al = 0.11; Fig. 2) in the summertime (December–February) and lower Fe / Al and Ti / Al ratios closer to the average UCC ratios (Fe / Al = 0.435 and Ti / Al = 0.05; McLennan, 2001) in wintertime (June–August; Fig. 2). Summertime Fe / Al ratios in kunanyi / Mount Wellington aerosols were slightly higher (Fe / Al = 0.72) than the Australian soil measurements. This can be explained by increased contribution of local soil emission from Tasmania under drier weather conditions as the NGSA database shows a higher Fe / Al ratio (on average 0.7, $n = 21$ samples) in Tasmanian soil compared to other soil across Australia (de Caritat and Cooper, 2011; de Caritat, 2022). While enhanced air masses originating from the Australian mainland cannot be observed in the summertime using the Hybrid Single-Particle Lagrangian Integrated Trajectory (HYSPLIT; Stein et al., 2015) model (Fig. S1), the Australian Bureau of Meteorology reports increasing southward-blowing winds at our sampling station from January through to March (Fig. S2). Such discrepancies emphasise the complex regional wind pattern influencing our sampling station and highlight the need to consider other parameters such as seasonal changes in environmental conditions at the source region when investigating aerosol entrainment and transport. Ti / Al ratios were found to lie between our Australian soil (Ti / Al = 0.11) and UCC (Ti / Al = 0.05) references from December through to May and then fell below the UCC ratio in the cooler months of the year. This monthly variability indicates that different lithogenic sources of Fe and Ti are likely to influence the atmospheric loading at our sampling station throughout the year. The onset of the dust season on the Australian mainland (October–November; Baddock et al., 2015) may explain part of the summer (dusty) season atmospheric inputs at our kunanyi / Mount Wellington aerosol sampling station, as evidenced by higher Fe / Al (and Ti / Al) ratios in aerosols. On the other hand, other atmospheric sources (locally derived from Tasmania or from long-range transport over the Southern Ocean) with a similar (lower) metal / Al signature than the UCC seem to prevail in our study region during winter. However, the small number of aerosol samples available between May–October in our study does not allow for accurate assessment of trends during the winter period. Much smaller variability was observed for the Th / Al ratio calculated in kunanyi / Mount Wellington aerosols (mean Th / Al = 0.00017) across the time series, with an overall median ratio close to that of the UCC (mean
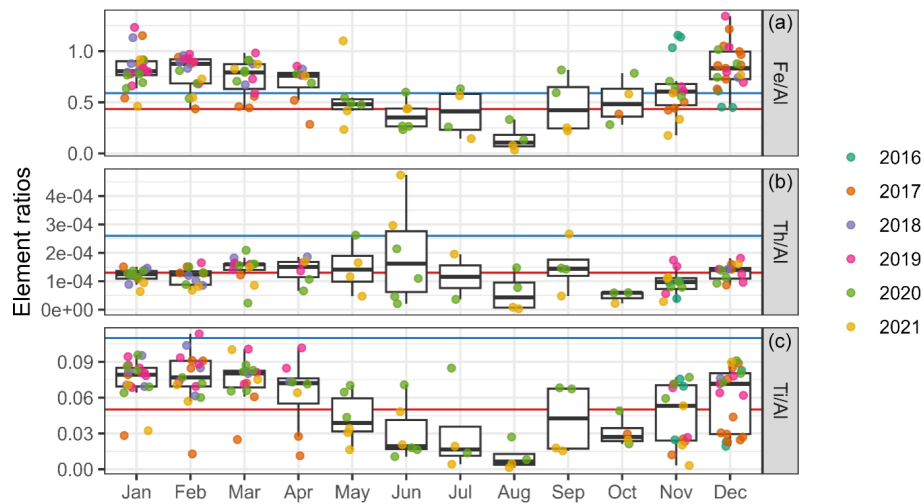
Figure 2. Boxplot of elemental ratios of Fe / Al **(a)**, Th / Al **(b)**, and Ti / Al **(c)** in kunanyi / Mount Wellington aerosol samples collected between 2016–2021, grouped according to month. Whiskers represent 1.5 times the interquartile range (75th–25th percentile) beyond the boxes, while the upper, middle, and lower horizontal lines of the box represent the higher interquartile, median value, and lower interquartile of the average monthly dataset, respectively. Colours represent each sample collection year. Horizontal red lines represent metal ratios in the average UCC (McLennan, 2001). Horizontal blue lines represent average metal ratios in the 11 selected NGSA Australian soil samples (this study). Two Th outliers (May and June 2020) were excluded from the Th dataset and subsequent calculation for clarity.

Th / Al $= 0.00013$) across most of the year, except during August and October.

Differences between elemental ratios in soil and in aerosol samples may stem from atmospheric processes occurring during transport between source regions and the sampling site, including the preferential settling of denser (e.g. oxyhydroxides) minerals over lighter minerals (e.g. clay) and from the mixing of different lithogenic air masses during atmospheric transport. Analysis of a large set of soil samples, including more locations across Australia and particularly in Tasmania, as well as high-resolution information on wind speed and direction at the sampling site and for the duration of the time series, is necessary to better assess the relative contribution of different Australian dust sources to the lithogenic particulate loading at kunanyi / Mount Wellington.

3.2 Single-tracer lithogenic particle fluxes at kunanyi / Mount Wellington: characteristics and trends

Thorium and Ti are commonly used as tracers of lithogenic atmospheric deposition fluxes as they are almost exclusively derived from lithogenic material and have little reactivity or biological utility in the atmosphere (Boës et al., 2011; Ohnemus and Lam, 2015). While Al may be emitted to the atmosphere by anthropogenic sources, its prevailing source in the offshore atmosphere remains crustal material (Xu and Weber, 2021). Although Fe solubility varies following physicochemical processes during the atmospheric transport, the soluble Fe fraction remains small compared to the total (mostly refractory) fraction of Fe delivered by dust. Hence, if all four

tracers have a unique lithogenic source, the use of a multiple tracer lithogenic flux estimate can reduce the uncertainty associated with the variability in a single metal's concentration due to contamination, deviation from the UCC, or secondary atmospheric inputs (Traill et al., 2022).

A strong correlation (mostly $R^2 > 0.8$) was found between the total atmospheric concentrations of Al, Fe, Th, and Ti in the individual samples (Table 2). The strongest correlation ($R^2 = 0.90$) was found between Al and Th, and the weakest correlation ($R^2 = 0.74$) was found between total Ti and Al concentrations in aerosols. Such strong correlations suggest that a common prevailing source may supply all four tracers to the kunanyi / Mount Wellington sampling station. Australian soil samples collected in the state of Victoria and analysed in this study also showed a good correlation between the four lithogenic tracers, with R^2 of 0.97, 0.74, and 0.73 for Fe, Th, and Ti when compared to Al (based on Table S4 data). Such a correlation was not found for soil samples from South Australia (only two soil samples from Western Australia). However, the small number of soil samples analysed in this study ($n = 4$ for Victoria and $n = 5$ in South Australia) is not sufficient to draw conclusions on the potential origin of metals in kunanyi / Mount Wellington aerosol samples. The NGSA database available from de Caritat and Cooper (2011) also shows a strong correlation (> 0.70) between Fe and Al measurements in soil samples from New South Wales, South Australia, and Tasmania using an aqua regia mineralisation and X-ray fluorescence analysis protocol.

Dust deposition fluxes estimated using individual tracer (Al, Fe, Th, and Ti) concentrations measured in kunanyi / Mount Wellington aerosols, called $F_{\text{Lith}(X)}$, showed
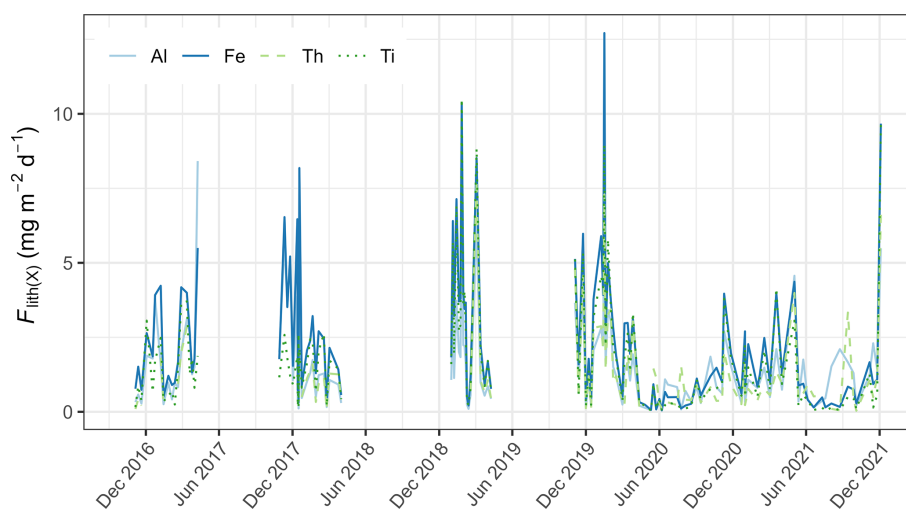
Figure 3. Individual tracer flux, $F_{\text{Lith}(X)}$ (mg m^{-2} d^{-1}), at the kunanyi / Mount Wellington aerosol sampling station from 2016 to 2021. Data points represent each aerosol mid-sampling period. Gaps in the time series are periods where samples were not collected due to logistical limitations (winter) or instrument maintenance. Here, $F_{\text{Lith}(X)}$ values are calculated using the average UCC content for each metal, as reported in McLennan (2001).

Table 2. Correlation coefficient (R^2) between tracer concentrations in kunanyi / Mount Wellington aerosols.

	Al	Th	Fe	Ti
Al	1	–	–	–
Th	0.90	1	–	–
Fe	0.87	0.82	1	–
Ti	0.74	0.84	0.83	1

similar variability throughout the time series (2016–2021; Fig. 3). Overall, the smallest $F_{\text{Lith}(Th)}$ flux was estimated using Th as a single lithogenic tracer, ranging between 0.03 and 7.8 mg m^{-2} d^{-1}. The largest dust flux was obtained using Fe as a lithogenic tracer and ranged between 0.05 and 12.7 mg m^{-2} d^{-1} ($F_{\text{Lith}(Fe)}$; Fig. 3). Lithogenic flux estimates calculated using Al and Ti concentrations in aerosols ranged from 0.06–8.4 mg m^{-2} d^{-1} and from 0.03–10.5 mg m^{-2} d^{-1} for $F_{\text{Lith}(Al)}$ and $F_{\text{Lith}(Ti)}$, respectively. Despite slight differences found between $F_{\text{Lith}(X)}$ estimates obtained using different lithogenic tracers, the magnitude of the difference between the highest and lowest $F_{\text{Lith}(X)}$ estimates varied by only a factor of 2, which reinforces the likelihood of a common prevailing atmospheric source for all four tracers.

This finding corroborates work presented by Traill et al. (2022), where concentrations of all four lithogenic tracers showed similar variabilities in marine sinking particles collected in the subantarctic region of the Southern Ocean south of Tasmania (SOTS station). Similarly, Traill et al. (2022) estimated higher lithogenic fluxes when using Fe as a lithogenic tracer and lower lithogenic fluxes when using Th as a lithogenic tracer (Traill et al., 2022). Median $F_{\text{Lith}(X)}$

estimates measured at the kunanyi / Mount Wellington sampling site (this study: 1.2, 1.7, 0.8, and 1.1 mg m^{-2} d^{-1} using Al, Fe, Th, and Ti as individual lithogenic tracers, respectively) compare well with reported dust deposition fluxes of 1.4–5 mg m^{-2} d^{-1} estimated by models in the study region (Jickells et al., 2005; Mahowald et al., 2005; Weis et al., 2024) and other Southern Hemisphere dust fluxes < 2.7 mg m^{-2} d^{-1} reported off the coasts of southern Africa and South America, away from major dust sources (Menzel Barraqueta et al., 2019). Our flux estimates are smaller than the mineral dust deposition estimates of 4.0–25.0 mg m^{-2} d^{-1} (based on Ti concentration in aerosols) reported by Strzelec et al. (2020a) in Western Australia, which is much closer to large Australian deserts.

Overall, maximum $F_{\text{Lith}(X)}$ estimates in our study were calculated during austral summer months (roughly December–March). Different metals are observed to dominate the summer $F_{\text{Lith}(X)}$ peak each year, with Al showing the highest $F_{\text{Lith}(X)}$ flux in summer 2016/2017 (8.4 mg m^{-2} d^{-1}), Fe in 2017/2018 (8.2 mg m^{-2} d^{-1}) and in 2019/2020 (12.7 mg m^{-2} d^{-1}), and Ti in 2018/2019 (10.5 mg m^{-2} d^{-1}) and in 2021/2022 (9.6 mg m^{-2} d^{-1}). This may be due to variabilities in the nature and composition of the dominant dust source arriving at the sampling site each year, including the impact of dust-containing fire emissions during the summer seasons of 2018/2019 and 2019/2020 (Perron et al., 2022).

3.3 Multi-tracer particle flux

All four tracers (Al, Fe, Th, and Ti) measured in kunanyi / Mount Wellington aerosols showed a strong correlation with one another and a similar variability over time

(Sect. 3.1), suggesting that they originated from a single terrestrial source. This supports the approach taken in this study, whereby a multi-tracer lithogenic deposition flux, called F_{LithAv}, is estimated by averaging $F_{\mathrm{Lith}(X)}$ fluxes obtained using each of the four tracers for each sample. The resulting F_{LithAv} estimated at our station between 2016 and 2021 is displayed in Fig. 4 and provides a more robust estimate of the deposition flux by smoothing variability between tracers (displayed in Fig. 3). Individual and average lithogenic flux estimates ($F_{\mathrm{Lith}(X)}$ and F_{LithAv}, respectively) calculated in this study are summarised for individual samples in Tables S5 and S6, respectively.

A mean F_{LithAv} value of $1.8 \pm 1.3\,\mathrm{mg\,m^{-2}\,d^{-1}}$ was calculated based on the analysis of aerosol samples collected between 2016 and 2021 at kunanyi / Mount Wellington (Tasmania; Fig. 4 – orange colour). Throughout our time series, the highest F_{LithAv} values were observed in January 2019 and 2020, with flux peaks reaching 9.2 in January 2019 and $9.0\,\mathrm{mg\,m^{-2}\,d^{-1}}$ in January 2020, respectively. Noticeable peak fluxes of $7.9\,\mathrm{mg\,m^{-2}\,d^{-1}}$ also occurred in early March 2019 and in mid-December 2021. Extended periods of low F_{LithAv} estimates ($0.5\,\mathrm{mg\,m^{-2}\,d^{-1}}$) were observed during the two austral winter periods sampled, with a minimum flux of $0.06\,\mathrm{mg\,m^{-2}\,d^{-1}}$ reached in May 2020 (Fig. 4). There is therefore an apparent seasonal trend in dust deposited at the kunanyi / Mount Wellington site, with higher F_{LithAv} observed in warmer periods (November–March) and lower fluxes in cooler periods of the year (May–August). It should be mentioned that a mean F_{LithAv} value of $2.7 \pm 1.9\,\mathrm{mg\,m^{-2}\,d^{-1}}$ is estimated when using the average metal content in Australian soil analysed in this study (Fig. 4 – green colour). Indeed, while Th and Ti contained in our 11 Australian soil samples show similar concentrations (within 10 %) to those in the average UCC (McLennan, 2001), Al and Fe concentrations in these local soil samples differ by 52 % and 35 %, respectively. This result in higher F_{LithAv} estimated using Australian soil data (Fig. 4).

The mean F_{LithAv} observed in this study, of $1.8\,\mathrm{mg\,m^{-2}\,d^{-1}}$ when using the average UCC and $2.7\,\mathrm{mg\,m^{-2}\,d^{-1}}$ when using the average Australian soil measurement (Table S5), falls within the dust deposition range of 1.1–$5.5\,\mathrm{mg\,m^{-2}\,d^{-1}}$ reported by models in southeastern Australia, which account for soil erodibility, soil particle size distribution, and wind friction velocity (Albani et al., 2014; Weis et al., 2024). In the Southern Ocean south of Tasmania, smaller mineral dust fluxes of 0.37 and $1.0\,\mathrm{mg\,m^{-2}\,d^{-1}}$ were reported based on aerosol Fe measurements at sea, particle size, and surface wind speed (Bowie et al., 2009), based on Al, Fe, Th, and Ti measurements in marine sinking particles (Traill et al., 2022), respectively. Traill et al. (2022) reported a similar annual variability in lithogenic deposition flux at SOTS between 2011 and 2018, with minimum F_{LithAv} around $0.5\,\mathrm{mg\,m^{-2}\,d^{-1}}$ in July–September and an earlier dust deposition peak (compared to our study) in November–December of up to $2.5\,\mathrm{mg\,m^{-2}\,d^{-1}}$.

Strzelec et al. (2020a) also reported (up to 6 times) higher mineral dust fluxes in warmer months compared to cooler months, based on Ti analysis in aerosols from Western Australia. In particular, the two summer seasons showing F_{LithAv} over $9.0\,\mathrm{mg\,m^{-2}\,d^{-1}}$ correspond to large bushfire seasons in Tasmania and in the Australian mainland upwind of Tasmania, respectively (Perron et al., 2022). Indeed, fire events are known to exacerbate dust entrainment into the atmosphere both during (pyroconvective updrafts) and after (burnt ground) fire events (Hamilton et al., 2022). It is worth noting that F_{LithAv} estimated using Australian soil measurements (this study) falls closer to the mean reported estimate found in the literature, while using the average UCC value results in a lower-end F_{LithAv} estimate compared to the literature. While F_{LithAv} estimated using the average UCC may present an advantage in that it is more comparable with other studies worldwide, F_{LithAv} estimated using Australian soil data may be more relevant for validating model outputs as it likely better represents true deposition fluxes in our study region. Overall, the choice of one or the other crustal source results in a difference of up to a factor of 2 in the calculated F_{LithAv}.

The greatest F_{LithAv} fluxes are annually observed during the austral summer (December–March), with median F_{LithAv} values of $2.4\,\mathrm{mg\,m^{-2}\,d^{-1}}$ in January and around $1.4\,\mathrm{mg\,m^{-2}\,d^{-1}}$ in December, February, and March across all years (Fig. 5). This tendency aligns with higher frequency of dust storms occurring in Australia's main geological basins during warmer months (late austral spring and summer), resulting in higher dust deposition fluxes (O'Loingsigh et al., 2017). The summers of 2017/2018 (November–December), 2018/2019 (January–February), and 2019/2020 (December–February) had especially high F_{LithAv} fluxes compared to other summer periods in the time series (Fig. 5). These observations are consistent with the year 2017 being identified as the third driest year since records have been kept in Australia (Steffen et al., 2018) and the two following summer periods being identified as strong bushfire years across Tasmania in 2018/2019 and across southeast Australia in 2019/2020 (Perron et al., 2022). Relatively smaller peaks were observed during the summer of 2020/2021 and, to a lesser extent, during the 2016/2017 summer (Fig. 5). This may reflect two wetter summer periods under the influence of El Niño–Southern Oscillation positive phase (La Niña), where increased moisture in the topsoil restricted particles from being eroded and entrained by air masses (Bureau of Meteorology, 2022). In addition, fewer bushfire emissions during these two wetter summer periods may have resulted in fewer dust emissions due to increased vegetation cover on the soil (Bureau of Meteorology, 2022). Wetter summer seasons may also explain a shift in F_{LithAv} peaks towards the end of the summer seasons in 2016/2017 and 2020/2021 (February–March) compared to the December–January F_{LithAv} peak observed in 2017/2018, 2018/2019, and 2019/2020 (Fig. 5).
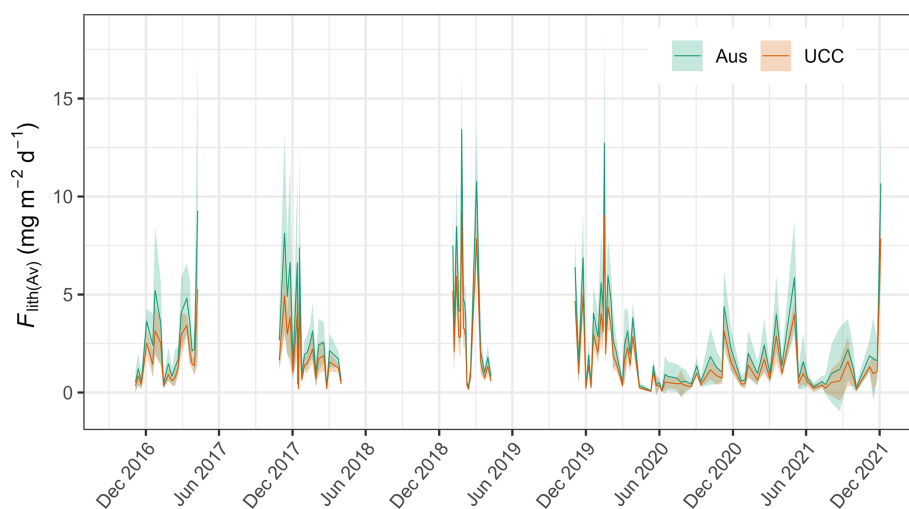
Figure 4. Multi-tracer lithogenic flux estimate, F_{LithAv} (expressed in $mg\,m^{-2}\,d^{-1}$), corresponding to the average of all individual tracer fluxes ($F_{Lith(X)}$) calculated based on the lithogenic composition of the UCC (orange colour) and that of the 11 Australian soil samples measured in this study (green colour). Shadings represent approximately one F_{LithAv} standard deviation of the average (solid lines).
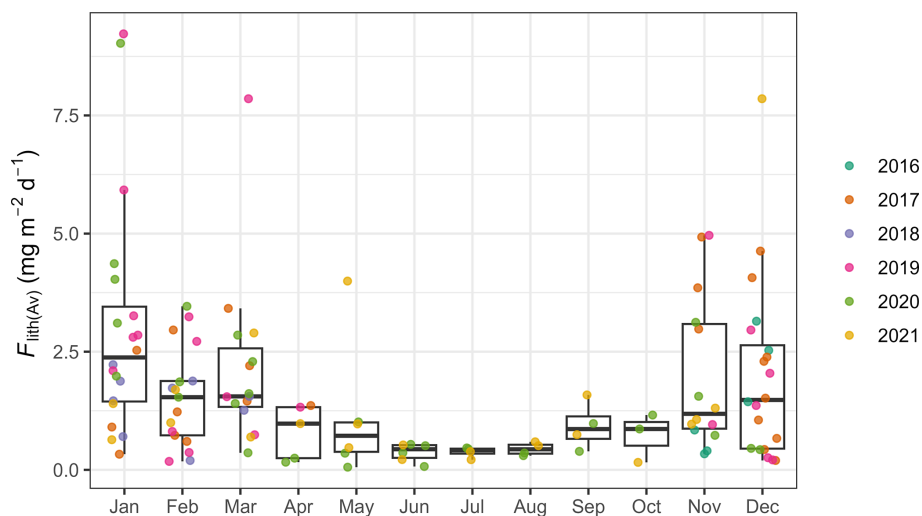

Figure 5. Monthly F_{LithAv} estimates (in $mg\,m^{-2}\,d^{-1}$) based on lithogenic tracer analysis in aerosol samples collected between 2016–2021 at the kunanyi / Mount Wellington site. Individual (weekly) samples are shown as dots, and the colour code represents each collection year. Whiskers represent 1.5 times the interquartile range (75th–25th percentile) beyond the boxes, while the upper, middle, and lower horizontal lines of the box represent the higher interquartile, median value, and lower interquartile of the average monthly dataset, respectively.

4　Conclusions

This study explores the seasonal and interannual variability in the lithogenic deposition flux using analysis of Al, Fe, Th, and Ti (as lithogenic tracers) in aerosol samples collected at kunanyi / Mount Wellington (Tasmania, Australia). Enrichment factors close to 1 and elemental ratios similar to those measured in soil samples collected in Australian dust source regions confirmed the crustal origin of all four tracers. Deposition fluxes, $F_{Llith(X)}$, calculated using each tracer individually showed small differences, of a factor 2 on average, between one another throughout the 2016–2021 time series.

This study suggests the use of a multi-tracer (averaged) dust deposition flux estimate as a more robust method to account for variability in individual tracers in aerosols.

The mean F_{LithAv} of $1.8\,mg\,m^{-2}\,d^{-1}$ calculated in this study across the 2016–2021 time series is consistent with earlier lithogenic deposition fluxes reported in the literature. Dust flux maxima (up to $9.2\,mg\,m^{-2}\,d^{-1}$) were consistently observed during the austral summer, while minimum annual F_{LithAv} (down to $0.06\,mg\,m^{-2}\,d^{-1}$) were estimated in the winter. Overall, individual year F_{LithAv} fluxes aligned well with the occurrence of known dust and bushfire events in the summertime, as well as other global meteorological events

such as the El Niño–Southern Oscillation (ENSO) which drive the weather patterns across southeast Australia.

Dust deposition fluxes calculated in this study hold some uncertainties (a factor of 3 and a factor of 2) due to the use of a set deposition velocity and the assumption of metal abundance as per the average UCC, respectively. While using the averaged UCC to calculate F_{LithAv} may present an advantage in being more comparable with other studies worldwide, we show that F_{LithAv} estimates (0.09–13.4 mg m^{-2} d^{-1}) calculated using metal abundance in Australian soils are in better agreement with dust fluxes reported by global models in our study region. Therefore, understanding local soil composition is essential to estimating dust deposition fluxes in different study regions. Overall, the uncertainty in field-based dust deposition flux estimates likely remain smaller than uncertainties associated with model parameterisation.

As dust deposition is now being recognised as a major source of vital micro-nutrients such as Fe to the Southern Ocean, accurately quantifying dust fluxes is vital to understanding primary production in the Southern Ocean and how this may change under future climate scenarios. Our observed dust flux maxima in austral summer may also provide a much-needed regional pulse of nutrients to phytoplankton when water column nutrients are being depleted through the growing season. Additional observations covering a wider geographical area and greater temporal coverage (including time series stations and winter sampling periods) are required to better constrain seasonal and interannual variability. Our study adds vital data to the relatively few field-based dust deposition flux estimates available to validate model outputs, especially for Southern Hemisphere dust sources (including Australia), which greatly vary in nature and composition.

Data availability. All data produced in this study are available either in the paper (Tables 1 and 2) or in the Supplement (Tables S1 to S6).

Supplement. The supplement related to this article is available online at: https://doi.org/10.5194/ar-2-315-2024-supplement.

Author contributions. ARB was responsible for the project conceptualisation, funding acquisition, resources, and supervision. MMGP was responsible for part of the sample collection, sample processing, data interpretation, processing, and curation, as well as writing the draft. SM was responsible for part of the sample collection and analysis and for laboratory supervision. TMH was responsible for data curation. CN was responsible for the analysis of soil samples. CH was responsible for part of the sample collection, sample processing, data curation, and writing the original draft. ATT was responsible for the instrument analysis. PdC was responsible for part of the sample collection and data curation. MS was responsible for part of the sample collection and sample processing. All authors were responsible for data interpretation and validation and reviewing and editing the paper.

Acknowledgement to country. Before the white settlement of lutruwita / Tasmania, kunanyi / Mount Wellington was a prominent feature in the lives of the Moomairremener people for thousands of years and continues to be today. We pay our respects to elders past, present, and emerging and are thankful to have been able to study this region.

Disclaimer. Publisher's note: Copernicus Publications remains neutral with regard to jurisdictional claims made in the text, published maps, institutional affiliations, or any other geographical representation in this paper. While Copernicus Publications makes every effort to include appropriate place names, the final responsibility lies with the authors.

Special issue statement. This article is part of the special issue "RUSTED: Reducing Uncertainty in Soluble aerosol Trace Element Deposition (*AMT/ACP/AR/BG* inter-journal SI)". It is not associated with a conference.

Review statement. This paper was edited by Benjamin Murray and reviewed by Zongbo Shi and one anonymous referee.

References

Albani, S., Mahowald, N. M, Perry, A. T., Scanza, R. A., Zender, C. S., Heavens, N. G., Maggi, V., Kok, J. F., and Otto-Bliesner, B. L.: Improved dust representation in the Community Atmosphere Model, J. Adv. Model. Earth Sy., 6, 541–570, https://doi.org/10.1002/2013MS000279, 2014.

Anderson, R. F., Cheng, H., Edwards, R. L., Fleisher, M. Q., Hayes, C. T., Huang, K.-F., Kadko, D., Lam, P. J., Landing, W. M., Lao, Y., Lu, Y., Measures, C. I., Moran, S. B., Morton, P. L., Ohnemus, D. C., Robinson, L. F., and Shelley, R. U.: How well can we quantify dust deposition to the ocean?, Philos. T. R. Soc. A, 374, 20150285, https://doi.org/10.1098/rsta.2015.0285, 2016.

Baddock, M., Parsons, K., Strong, C., Leys, J., and McTainsh, G.: Drivers of Australian dust: a case study of frontal winds and dust dynamics in the lower lake Eyre basin, Earth Surf. Process., 40, 1982–1988, https://doi.org/10.1002/esp.3773, 2015.

Baker, A. R., Landing, W. M., Bucciarelli, E., Cheize, M., Fietz, S., Hayes, C. T., Kadko, D., Morton, P. L., Rogan, N., Sarthou, G., Shelley, R. U., Shi, Z., Shiller, A., and van Hulten M. M. P.: Trace element and isotope deposition across the air–sea interface: progress and research needs, Philos. T. R. Soc. A, 374, 20160190, https://doi.org/10.1098/rsta.2016.0190, 2016.

Baker, A. R., Kanakidou, M., Altieri, K. E., Daskalakis, N., Okin, G. S., Myriokefalitakis, S., Dentener, F., Uematsu, M., Sarin, M. M., Duce, R. A., Galloway, J. N., Keene, W. C., Singh, A., Zamora, L., Lamarque, J.-F., Hsu, S.-C., Rohekar, S. S., and Prospero, J. M.: Observation- and model-based estimates of particulate dry nitrogen deposition to the oceans, Atmos. Chem. Phys., 17, 8189–8210, https://doi.org/10.5194/acp-17-8189-2017, 2017.

Baker, A. R., Li, M., and Chance, R.: Trace metal fractional solubility in size-segregated aerosols from the tropical eastern Atlantic Ocean, Global Biogeochem. Cy., 34, e2019GB006510, https://doi.org/10.1029/2019GB006510, 2020.

Bindu, G., Nair, P. R., Aryasree, S., Hegde, P., and Salu Jacob, S.: Pattern of aerosol mass loading and chemical composition over the atmospheric environment of an urban coastal station, J. Atmos. Sol.-Ter. Phy., 138, 121–135, https://doi.org/10.1016/j.jastp.2016.01.004, 2016.

Boës, X., Rydberg, J., Martinez-Cortizas, A., Bindler, R., and Renberg, I., Evaluation of conservative lithogenic elements (Ti, Zr, Al, and Rb) to study anthropogenic element enrichments in lake sediments, J. Paleolimnol., 46, 75–87, https://doi.org/10.1007/s10933-011-9515-z, 2011.

Bowie, A. R., Lannuzel, D., Remenyi, T. A., Wagener, T., Lam, P. J., Boyd, P. W., Guieu, C., Townsend, A. T., and Trull, T. W.: Biogeochemical iron budgets of the Southern Ocean south of Australia: Decoupling of iron and nutrient cycles in the subantarctic zone by the summertime supply, Global Biogeochem. Cy., 23, GB4034, https://doi.org/10.1029/2009GB003500, 2009.

Bowler, J. M.: Aridity in Australia: Age, origins and expression in aeolian landforms and sediments, Earth-Sci. Rev., 12, 279–310, https://doi.org/10.1016/0012-8252(76)90008-8, 1976.

Bureau of Meteorology: ENSO Outlook, http://www.bom.gov.au/climate/enso/outlook (last access: 28 November 2024), 2022.

Crawford, J., Cohen, D. D., Atanacio, A., Manohar, M., and Siegele, R.: Fingerprinting Australian soils based on their source location, Atmos. Pollut. Res., 12, 173–183, https://doi.org/10.1016/j.apr.2021.01.007, 2021.

Cudahy, T., Caccetta, M., Thomas, M., Hewson, R., Abrams, M., Kato, M., Kashimura, O., Ninomiya, Y., Yamaguchi, Y., Collings, S., Laukamp, C., Ong, C., Lau, I., Rodger, A., Chia, J., Warren, P., Woodcock, R., Fraser, R., Rankine, T., Vote, J., de Caritat, P, English, P., Meyer, D., Doescher, C., Fu, B., Shi, P., and Mitchell, R.: Satellite-derived mineral mapping and monitoring of weathering, deposition and erosion, Sci. Rep., 6, 23702, https://doi.org/10.1038/srep23702, 2016.

Cutter, G. A., Casciotti, K., Croot, P., Geibert, W., Heimbürger, L.-E., Lohan, M. C., Planquette, H., and van de Flierdt, T.: Sampling and Sample-handling Protocols for GEOTRACES Cruises, Version 3.0, Bremerhaven, GEOTRACES Standards and Intercalibration Committee, https://geotracesold.sedoo.fr/images/Cookbook.pdf (last access: 28 Noveber 2024), 2017.

de Caritat, P.: The National Geochemical Survey of Australia: review and impact, Geochem.-Explor. Env. A, 22, geochem2022-032, https://doi.org/10.1144/geochem2022-032, 2022.

de Caritat, P. and Cooper, M.: National Geochemical Survey of Australia: The Geochemical Atlas of Australia, Record 2011/020, Geoscience Australia, Canberra, https://doi.org/10.11636/Record.2011.020, 2011.

De Deckker, P.: An evaluation of Australia as a major source of dust, Earth-Sci. Rev., 194, 536–567, https://doi.org/10.1016/j.earscirev.2019.01.008, 2019.

Duce, R. A., Liss, P. S., Merrill, J. T., Atlas, E. L., BuatMenard, P., Hicks, B. B., Miller, J. M., Prospero, J. M., Arimoto, R., Church, T. M., Ellis, W., Galloway, J. N., Hansen, L., Jickells, T. D., Knap, A. H., Reinhardt, K. H., Schneider, B., Soudine, A., Tokos, J. J., Tsunogai, S., Wollast, R., and Zhou, M.: The atmospheric input of trace species to the world ocean, Global Biogeochem. Cy., 5, 193–259, https://doi.org/10.1029/91GB01778, 1991.

Hamilton, D. S., Perron, M. M. G., Bond, T. C., Bowie, A. R., Buchholz, R. R., Guieu, C., Ito, A., Maenhaut, W., Myriokefalitakis, S., Olgun, N., Rathod, S. D., Schepanski, K., Tagliabue, A., Wagner, R., and Mahowald, N. M.: Earth, Wind, Fire, and Pollution: Aerosol Nutrient Sources and Impacts on Ocean Biogeochemistry, Annu. Rev. Mar. Sci., 14, 303–330, https://doi.org/10.1146/annurev-marine-031921-013612, 2022.

Ito, A., Perron, M. M. G., Proemse, B. C., Strzelec, M., Gault-Ringold, M., Boyd, P. W., and Bowie, A. R.: Evaluation of aerosol iron solubility over Australian coastal regions based on inverse modeling: implications of bushfires on bioaccessible iron concentrations in the Southern Hemisphere, Prog. Earth Planet. Sci., 7, 42, https://doi.org/10.1186/s40645-020-00357-9, 2020.

Jickells, T., An, Z. S., Andersen, K. K., Baker, A. R., Bergametti, G., Brooks, N., Cao, J. J., Boyd, P. W., Duce, R. A., Hunter, K. A., Kawahata, H., Kubilay, N., Laroche, J., Liss, P. S., Mahowald, N., Prospero, J. M, Ridgwell, A. J., Tegen,

I., and Torres, R.: Global Iron Connections Between Desert Dust, Ocean Biogeochemistry, and Climate, Science, 308, 67–71, https://doi.org/10.1126/science.1105959, 2005.

Mackie, D. S., Boyd, P. W., McTainsh, G. H., Tindale, N. W., Westberry, T. K., and Hunter, K. A.: Biogeochemistry of iron in Australian dust: From eolian uplift to marine uptake, Geochem. Geophy. Geosy., 9, Q03Q08, https://doi.org/10.1029/2007GC001813, 2008.

Mahowald, N. M., Baker, A. R., Bergametti, G., Brooks, N., Duce, R. A., Jickells, T. D., Kubilay, N., Prospero, J. M., and Tegen, I.: Atmospheric global dust cycle and iron inputs to the ocean, Global Biogeochem. Cy., 19, GB4025, https://doi.org/10.1029/2004GB002402, 2005.

Mahowald, N. M., Engelstaedter, S., Luo, C., Sealy, A., Artaxo, P., Benitez-Nelson, C., Bonnet, S., Chen, Y., Chuang, P. Y., Cohen, D. D., Dulac, F., Herut, B., Johansen, A. M., Kubilay, N., Losno, R., Maenhaut, W., Paytan, A., Prospero, J. M., Shank, L. M., and Siefert, R. L.: Atmospheric Iron Deposition: Global Distribution, Variability, and Human Perturbations, Ann. Rev. Mar. Sci., 1, 245–278, https://doi.org/10.1146/annurev.marine.010908.163727, 2009.

McLennan, S. M.: Relationships between the trace element composition of sedimentary rocks and upper continental crust, Geochem. Geophy. Geosy., 2, 2000GC000109, https://doi.org/10.1029/2000GC000109, 2001.

Menzel Barraqueta, J.-L., Klar, J. K., Gledhill, M., Schlosser, C., Shelley, R., Planquette, H. F., Wenzel, B., Sarthou, G., and Achterberg, E. P.: Atmospheric deposition fluxes over the Atlantic Ocean: a GEOTRACES case study, Biogeosciences, 16, 1525–1542, https://doi.org/10.5194/bg-16-1525-2019, 2019.

Morton, P. L., Landing, W. M., Hsu, S.-C., Milne, A., Aguilar-Islas, A. M., Baker, A. R., Bowie, A. R., Buck, C. S., Gao, Y., Gichuki, S., Hastings, M. G., Hatta, M., Johansen, A. M., Losno, R., Mead, C., Patey, M. D., Swarr, G., Vandermark, A., and Zamora, L. M.: Methods for the sampling and analysis of marine aerosols: results from the 2008 GEOTRACES aerosol intercalibration experiment, Limnol. Oceanogr.-Meth., 11, 62–78, 2013.

Ohnemus, D. C. and Lam, P. J.: Cycling of lithogenic marine particles in the US GEOTRACES North Atlantic transect, Deep-Sea Res. Pt. II, 116, 283–302, https://doi.org/10.1016/j.dsr2.2014.11.019, 2015.

O'Loingsigh, T., Chubb, T., Baddock, M., Kelly, T., Tapper, N. J., De Deckker, P., and McTainsh, G.: Sources and pathways of dust during the Australian "Millennium Drought" decade, J. Geophys. Res.-Atmos., 122, 1246–1260, https://doi.org/10.1002/2016JD025737, 2017.

Perron, M. M. G., Strzelec, M., Gault-Ringold, M., Proemse, B. C., Boyd, P. W., and Bowie, A. R.: Assessment of leaching protocols to determine the solubility of trace metals in aerosols, Talanta, 208, 120377, https://doi.org/10.1016/j.talanta.2019.120377, 2020a.

Perron, M. M. G., Proemse, B. C., Strzelec, M., Gault-Ringold, M., Boyd, P. W., Sanz Rodriguez, E., Paull, B., and Bowie, A. R.: Origin, transport, and deposition of aerosol iron to Australian coastal waters, Atmos. Environ., 228, 117432, https://doi.org/10.1016/j.atmosenv.2020.117432, 2020b.

Perron, M. M. G., Proemse, B. C., Strzelec, M., Gault-Ringold, M., and Bowie, A. R.: Atmospheric inputs of volcanic iron around

Heard and McDonald Islands, Southern ocean, Environ. Sci., 1, 508–517, https://doi.org/10.1039/D1EA00054C, 2021.

Perron, M. M. G., Meyerink, S., Corkill, M., Strzelec, M., Proemse, B. C., Gault-Ringold, M., Sanz Rodriguez, E., Chase, Z., and Bowie, A. R.: Trace elements and nutrients in wildfire plumes to the southeast of Australia, Atmos. Res., 270, 106084, https://doi.org/10.1016/j.atmosres.2022.106084, 2022.

Potts, P. J., Thompson, M., Chenery, S. R., Webb, P. C., and Kasper, H. U.: GEOPT13 – an international proficiency test for analytical geochemistry laboratories – report on round 13/July 2003 (Koeln Loess)- International Association of Geoanalysts, https://geoanalyst.org/wp-content/uploads/2017/10/GeoPT13Report.pdf (last access: 3 December 2024), 2003.

Reimann, C. and de Caritat, P.: Distinguishing between natural and anthropogenic sources for elements in the environment: regional geochemical surveys versus enrichment factors, Sci. Total Environ., 337, 91–107, https://doi.org/10.1016/j.scitotenv.2004.06.011, 2005.

Shelley, R. U., Morton, P. L., and Landing, W. M.: Elemental ratios and enrichment factors in aerosols from the US-GEOTRACES North Atlantic transects, Deep-Sea Res. Pt. II, 116, 262–272, https://doi.org/10.1016/j.dsr2.2014.12.005, 2015.

Sprigg, R. C.: Some stratigraphic consequences of fluctuating Quaternary sea levels and related wind regimes in southern and central Australia, in: Quaternary dust mantles, China, New Zealand and Australia, edited by: Wasson, R. J., Australian National University, Canberra, 211–240, 1982.

Steffen, W., Rice, M., and Alexander, D.: Another record-breaking year for heat and extreme weather, Climate Council of Australia, ISBN 978-1-925573-47-3, 2018.

Stein, A. F., Draxler, R. R., Rolph, G. D., Stunder, B. J. B., Cohen, M. D., and Ngan, F.: NOAA's Hysplit Atmospheric Transport and Dispersion Modeling System, B. Am. Meteorol. Soc., 96, 2059–2077, https://doi.org/10.1175/Bams-D-14-00110.1, 2015.

Strzelec, M., Proemse, B. C., Barmuta, L. A., Gault-Ringold, M., Desservettaz, M., Boyd, P. W., Perron, M. M. G., Schofield, R., and Bowie, A. R.: Atmospheric Trace Metal Deposition from Natural and Anthropogenic Sources in Western Australia, Atmosphere-Basel, 11, 474, https://doi.org/10.3390/atmos11050474, 2020a.

Strzelec, M., Proemse, B. C., Gault-Ringold, M., Boyd, P. W., Perron, M. M. G., Schofield, R., Ryan, R. G., Ristovski, Z. D., Alroe, J., Humphries, R. S., Keywood, M. D., Ward, J., and Bowie, A. R.: Atmospheric Trace Metal Deposition near the Great Barrier Reef, Australia, Atmosphere-Basel, 11, 390, https://doi.org/10.3390/atmos11040390, 2020b.

Traill, C. D., Weis, J., Wynn-Edwards, C., Perron, M. M. G, Chase, Z., and Bowie, A. R.: Lithogenic Particle Flux to the Subantarctic Southern Ocean: A Multi-Tracer Estimate Using Sediment Trap Samples, Global Biogeochem. Cy., 36, e2022GB007391, https://doi.org/10.1029/2022GB007391, 2022.

Vecchio, M. A., Costas-Rodríguez, M., Caiazzo, L., Bruschi, F., Hobin, K., Vanhaecke, F., and Grotti, M.: Provenance of mineral dust deposited on Antarctica over the last sixty years by strontium isotopic analysis of snow from Dome C, Atmos. Environ., 338, 120850, https://doi.org/10.1016/j.atmosenv.2024.120850, 2024.

Weis, J., Schallenberg, C., Chase, Z., Bowie, A. R., Wojtasiewicz, B., Perron, M. M. G., Mallet, M. D., and Strutton, P. G.: South-

ern Ocean phytoplankton stimulated by wildfire emissions and sustained by iron recycling, Geophys. Res. Lett., 49, 1–11, https://doi.org/10.1029/2021GL097538, 2022.

Weis, J., Chase, Z., Schallenberg, C., Strutton, P. G, Bowie, A. R., and Fiddes, S. L.: One-third of Southern Ocean productivity is supported by dust deposition, Nature, 629, 603–608, https://doi.org/10.1038/s41586-024-07366-4, 2024.

Winton, V. H. L., Bowie, A. R., Edwards, R., Keywood, M., Townsend, A. T., van der Merwe, P., and Bollhöfer, A.: Fractional iron solubility of atmospheric iron inputs to the Southern Ocean, Mar. Chem., 177, 20–32, https://doi.org/10.1016/j.marchem.2015.06.006, 2016a.

Winton, V. H. L., Edwards, R., Bowie, A. R., Keywood, M., Williams, A. G., Chambers, S. D., Selleck, P. W., Desservettaz, M., Mallet, M. D., and Paton-Walsh, C.: Dry season aerosol iron solubility in tropical northern Australia, Atmos. Chem. Phys., 16, 12829–12848, https://doi.org/10.5194/acp-16-12829-2016, 2016b.

Xu, H. and Weber, T.: Ocean dust deposition rates constrained in a data-assimilation model of the marine aluminum cycle, Global Biogeochem. Cy., 35, e2021GB007049, https://doi.org/10.1029/2021GB007049, 2021.